Appl Microbiol Biotechnol
DOI 10.1007/s00253-013-5029-0

A new cytochrome P450 system from *Bacillus megaterium* DSM319 for the hydroxylation of 11-keto-β-boswellic acid (KBA)

Elisa Brill · Frank Hannemann · Josef Zapp · Gerit Brüning · Johann Jauch · Rita Bernhardt

Received: 15 March 2013 / Revised: 27 May 2013 / Accepted: 30 May 2013

Abstract In the genome of *Bacillus megaterium* DSM319, a strain who has recently been sequenced to fully exploit its potential for biotechnological purposes, we identified a gene encoding the cytochrome P450 CYP106A1 as well as genes encoding potential redox partners of CYP106A1. We cloned, expressed, and purified CYP106A1 and five potential autologous redox partners, one flavodoxin and four ferredoxins. The flavodoxin and three ferredoxins were able to support the activity of CYP106A1 displaying the first cloned natural redox partners of a cytochrome P450 from *B. megaterium*. The CYP106A1 system was able to convert the pentacyclic triterpene 11-keto-β-boswellic acid (KBA) belonging to the main bioactive constituents of *Boswellia serrata* gum resin extracts, which are used to treat inflammatory disorders and arthritic diseases. In order to provide sufficient amounts of the KBA products to characterize them structurally by NMR spectroscopy, recombinant whole-cell biocatalysts were constructed based on *B. megaterium* MS941. The main product has been identified as 7β-hydroxy-KBA, while the side product (~20 %) was shown to be a mixture of 7β,15α-dihydroxy-KBA and 15α-hydroxy-KBA. Without further optimization 560.7 mg l^{-1} day^{-1} of the main product, 7β-hydroxy-KBA, could be obtained thus providing a suitable starting point for the efficient production of modified KBA by chemical tailoring to produce novel KBA derivatives with increased bioavailability and this way more efficient drugs.

Keywords Cytochromes P450 · CYP106A1 · Flavodoxin · Ferredoxin · *Bacillus megaterium* · 11-Keto-β-boswellic acid

Electronic supplementary material The online version of this article (doi:10.1007/s00253-013-5029-0) contains supplementary material, which is available to authorized users.

E. Brill · F. Hannemann · R. Bernhardt
Department of Biochemistry, Saarland University, 66123 Saarbruecken, Germany

J. Zapp
Department of Pharmaceutical Biology, Saarland University, 66123 Saarbruecken, Germany

G. Brüning · J. Jauch
Department of Organic Chemistry II, Saarland University, 66123 Saarbruecken, Germany

R. Bernhardt (✉)
Institut für Biochemie, Universität des Saarlandes, Campus B.2.2, 66123 Saarbruecken, Germany
e-mail: ritabern@mx.uni-saarland.de

Introduction

Cytochromes P450 (CYPs and P450s) are a superfamily of heme containing external monooxygenases that can be found in all biological kingdoms (http://drnelson.uthsc.edu/CytochromeP450.html). The P450s mostly act as terminal monooxygenases as they activate molecular oxygen and integrate one oxygen atom into the substrate, while the other oxygen atom is reduced to water. The P450s are characterized by an extremely high diversity of the catalyzed reactions and the converted substrates (Bernhardt 2006). Due to this versatility, the cytochromes are involved in different biological processes like carbon source assimilation, carcinogenesis, the biosynthesis of steroid hormones, or the metabolism of drugs and xenobiotics (Bernhardt 1996; Werck-Reichhart and Feyereisen 2000; Urlacher and Eiben 2006; Bernhardt and Waterman 2007). This high diversity concerning the catalyzed reactions and converted substrates is the basis for the high biotechnological potential of P450s (Bernhardt 2006; Urlacher and Girhard 2012): Through the activity of P450s a plethora of substances can be produced whose chemical synthesis via, e.g., selective hydroxylations is both difficult and expensive. However, most cytochromes P450 are not able to interact directly with the external primary electron donor NAD(P)H, but one or two additional proteins are necessary

Published online: 25 June 2013

to transfer electrons from NAD(P)H to the P450. With respect of the protein components involved in the electron transfer reaction, the cytochrome P450 systems can be categorized into different classes (Hannemann et al. 2007). One of the main classes is the mitochondrial/bacterial type of the cytochrome P450 systems (class I), where the electrons are transferred from NAD(P)H via a FAD-containing ferredoxin reductase and a ferredoxin to the cytochrome P450. Concerning the ferredoxin component, [2Fe–2S] as well as non-[2Fe–2S] cluster ferredoxins have been found to support cytochrome P450 activity (Ewen et al. 2008), whereas the non-[2Fe–2S] cluster ferredoxins can be further divided into [3Fe–4S] and [4Fe–4S] cluster ferredoxins as well as dicluster ferredoxins containing a [3Fe–4S] and a [4Fe–4S] cluster or two [4Fe–4S] cluster. Class I P450 systems comprise most bacterial cytochromes, which are easy to purify and to handle because of their solubility. Besides, several other electron transfer systems exist (mainly in bacteria), which harbor other components like flavodoxins instead of ferredoxins or where different components of the cytochrome P450 system are joined to form fusion proteins (Hannemann et al. 2007). Flavodoxins are small electron transfer proteins (14–23 kDa) containing a tightly but noncovalently bound flavin mononucleotide as prosthetic group. They were first found in cyanobacteria (Smillie 1965) and clostridia (Knight et al. 1966) growing under low-iron conditions, where they substituted the iron-comprising ferredoxins in reactions resulting in N_2 and $NADP^+$ reduction (Sancho 2006). Besides these well-characterized functions, there are also flavodoxin-specific metabolic routes known in *Escherichia coli* and *Helicobacter pylori*, where flavodoxin is an essential, constitutive gene (Zheng et al. 1999; Puan et al. 2005; Freigang et al. 2002).

Bacillus megaterium is a Gram-positive, spore-forming, mainly aerobic bacterium. Its ability to grow on various carbon sources makes this organism an ideal industrial production host (Vary et al. 2007), which so far has been mainly used for the production of proteins. Among the products from *B. megaterium* are industrial enzymes like penicillin acyclase or different amylases, vitamins, and diagnostic enzymes (Vary et al. 2007). There are further reasons for the biotechnological and industrial interest in *B. megaterium*: It is not pathogen; it stably maintains plasmids and does not produce alkaline proteases thus being ideally applicable to produce homologous and heterologous proteins (Sussman et al. 1988; Meinhardt et al. 1989; Malten et al. 2005; Richhardt et al. 2010). Some of the most interesting proteins occurring in *B. megaterium* are cytochrome P450 monooxygenases (He and Fulco 1991). The self-sufficient cytochrome P450 BM3 from *B. megaterium* is the most investigated bacterial P450 so far, which has been used and redesigned to catalyze the oxidation of a variety of biotechnologically interesting substances (for review, see Whitehouse et al. 2012). The well-studied CYP106A2 from *B. megaterium* ATCC 13368 (Berg et al. 1976, 1979) is known to convert several biotechnologically interesting steroids (Virus et al. 2006; Nguyen et al. 2012; Zehentgruber et al. 2010) and terpenoic substances (Bleif et al. 2012; Schmitz et al. 2012). The genome of the *B. megaterium* strain ATCC 13368 has not been sequenced yet, and the natural redox partners of CYP106A2 have never been cloned. To date, no homologous redox partners of a cytochrome P450 from *B. megaterium* have been cloned. To fully exploit the potential of *B. megaterium*, the genomes of the strains QM B1551 and DSM319 have been sequenced (Eppinger et al. 2011).

In this study, we describe the identification and characterization of a CYP106A1 system from *B. megaterium* DSM319. We successfully expressed and purified the cytochrome P450 CYP106A1, one flavodoxin (Fld), one [2Fe–2S] cluster ferredoxin and three [3Fe–4S] or [4Fe–4S] cluster ferredoxins from *B. megaterium* DSM319. Fld and the three non-[2Fe–2S] cluster ferredoxins were found to functionally interact with the CYP106A1 supported by Arh1 from *Schizosaccharomyces pombe* as reductase. This heterologous cytochrome P450 system was applied in a whole-cell system to convert the pentacyclic triterpene 11-keto-β-boswellic acid (KBA) to 7β-hydroxy-KBA, 7β,15α-dihydroxy-KBA and 15α-hydroxy-KBA. These derivatives can be the basis for applying methods of synthetic biology to introduce additional modifications into this complex molecule for the production of more efficient drugs.

Materials and methods

Materials

KBA was isolated as described before (Jauch and Bergmann 2003). All other chemicals and reagents were of highest grade available.

Bioinformatic analysis

Genes encoding cytochromes P450 were searched in the *B. megaterium* DSM319 genome based on the heme-binding domain signature, FxxGx(H/R)xCxG as query sequence. Genes possessing such motifs were further examined for the presence of the highly conserved threonine in the potential I-helix and the conserved EXXR motif in the K-helix (Khatri et al. 2010). Putative flavodoxin and ferredoxin genes were identified by searching the *B. megaterium* DSM319 genome for genes similar to known flavodoxin and ferredoxin genes. The DNA sequences were translated using the ExPASy Translate tool. The Pfam database Version 24.0 was used to predict the ferredoxin cluster type (Finn et al. 2010).

Amplification and cloning of genes

For in vitro studies, genes encoding CYP106A1 (BMD_1855), the flavodoxin Fld (BMD_4866), Fdx1 (BMD_1901), Fdx2 (BMD_2329), Fdx3 (BMD_4349), and Fdx4 (BMD_0889) were amplified by polymerase chain reaction using genomic DNA of *B. megaterium* MS941 as template. The PCR primers were designed to introduce an *Nde*I restriction site at the 5′ end of the fragment and a *Hin*dIII restriction site with a 6-histidine tag at the 3′ end in case of CYP106A1, Fdx2, Fdx3, and Fdx4. The PCR primers for Fdx1 were designed to introduce an *Nde*I restriction site at the 5′ end of the fragment and a *Kpn*I restriction site with a 6-histidine tag at the 3′ end. The PCR primers for Fld were designed to introduce an *Nco*I restriction site at the 5′ end of the fragment and a *Bam*HI restriction site with a 6-histidine tag at the 3′ end. After subcloning of the resulting PCR products into the pCR4-TOPO vector (Invitrogen, San Diego, CA, USA), the plasmids were digested with the corresponding restriction enzymes and ligated into the previously linearized expression vector pET17b in case of CYP106A1 and the ferredoxins or pET3d in case of Fld.

For the *B. megaterium* whole-cell systems, all genes were cloned with an optimized ribosomal binding site for *B. megaterium* immediately upstream the coding regions. The genes encoding the flavodoxin and the ferredoxins were amplified by PCR from the pET3d or pET17b expression vectors constructed in this study and the PCR primers were designed to contain a *Sac*I restriction site at the 5′ end of the fragments and a *Not*I restriction site with a 6-histidine tag at the 3′ end for the ferredoxins or a *Bsr*GI restriction site at the 5′ end of the fragment and an *Sph*I restriction site at the 3′ end in case of Fld. After subcloning of the resulting PCR products in the pCR4-TOPO vector (Invitrogen, San Diego, CA, USA), they were digested with *Sac*I and *Not*I or *Bsr*GI and *Sph*I and ligated into the previously linearized pSMF2.1 vector (Bleif et al. 2012) yielding pSMF2.1Fld, pSMF2.1Fdx2, pSMF2.1Fdx3, and pSMF2.1Fdx4. The codon usage of Arh1 was optimized for the expression in *B. megaterium*, and the gene sequence was synthesized from Geneart including a *Kpn*I site and an optimized ribosomal binding site for *B. megaterium* immediately upstream the coding region and a *Sac*I site at the 3′ end. Arh1 was excised from this vector with *Kpn*I and *Sac*I and ligated upstream Fld or the ferredoxins into the previously constructed plasmids to yield pSMF2.1AFld, pSMF2.1AFdx2, pSMF2.1AFdx3, and pSMF2.1AFdx4. The gene encoding CYP106A1 was amplified by PCR from the pET17b expression vector constructed in this study and the PCR primers were designed to contain an *Spe*I restriction site at the 5' end of the fragment and a *Mlu*I restriction site at the 3′ end. The PCR-product was subcloned in the pCR4-TOPO vector (Invitrogen, San Diego, CA, USA) and digested with *Spe*I and *Mlu*I. The resulting fragment was inserted upstream Arh1 into the pSMF2.1 vectors containing Arh1 and Fld or one of the ferredoxins yielding the final expression vectors comprising CYP106A1, Arh1 and flavodoxin, Fdx2, Fdx3 or Fdx4: pSMF2.1BAFld, pSMF2.1BAFdx2, pSMF2.1BAFdx3 and pSMF2.1BAFdx4. A further vector was constructed by inserting only CYP106A1 in the pSMF2.1 vector without redox partners getting pSMF2.1B. Sequences of all constructed plasmids were verified by DNA-sequencing (Eurofins-MWG, Ebersberg, Germany).

Expression in *E. coli* and purification of the recombinant proteins

The expression of all *B. megaterium* proteins (CYP106A1, Fld, Fdx1, Fdx2, Fdx3, and Fdx4) was performed using *E. coli* C43(DE3) cells as expression host. The *E. coli* C43(DE3) cells were transformed with the corresponding expression plasmids and cultured overnight in terrific broth (TB) containing 100 μg/ml ampicillin at 37 °C and 150 rpm. This overnight culture was used to inoculate a 250 ml main culture in a 2-l baffled flask containing 100 μg/ml ampicillin, and the culture was grown at 37 °C and 100 rpm. When the OD_{600} reached 0.5, the cultures were induced by the addition of 1 mM isopropyl β-D-1-thiogalactopyranosid, while 0.5 mM delta-aminolevulinic acid was also added upon expression of CYP106A1 to support the heme synthesis. The cultures were grown at 28 °C and 100 rpm for 24 h. The *E. coli* cells were harvested by centrifugation at 4,500 rpm for 20 min, and the cell pellets were stored at −20 °C until further use. All purification steps were performed at 4 °C. The cell pellets were resuspended in 50 mM sodium phosphate buffer, pH 8.0 containing 300 mM NaCl and 50 μg/ml phenylmethylsulfonyl fluoride and disrupted by sonication. After centrifugation, the His_6-tagged proteins were purified by immobilized metal ion affinity chromatography using TALON™ resin (Clontech) according to the manufacturer's instructions. Fractions containing the heterologously expressed proteins were collected, concentrated by ultrafiltration and further purified by size exclusion chromatography using a Superdex 75 (GE Healthcare) column and 50 mM potassium phosphate buffer, pH 7.4, and a constant flow rate of 0.1 ml/min. Suitable fractions were collected, concentrated by ultrafiltration, and stored at −20 °C. The mutant Arh1_A18G from *S. pombe* showing increased yield of the holoprotein, named only Arh1 in this study, was expressed and purified as reported before (Ewen et al. 2008).

UV–visible absorbance spectroscopy

To analyze the spectral properties of the purified proteins, UV–visible absorbance spectra from 250 to 700 nm were recorded on a double-beam spectrophotometer (UV-2101PC, Shimadzu,

Japan). To determine the concentrations of Fld and the ferredoxins, the molar extinction coefficients at the characteristic maxima of the proteins were calculated using the concentrations obtained by the total protein quantification of the pure proteins using BC assay (Uptima/Interchim, Montlucon, France). The concentration of CYP106A1 was determined using CO-difference spectra and ΔA (450–490 nm)=91 mM^{-1} cm^{-1} referred to the method of Omura and Sato (1964).

Substrate-induced spin-state shifts

Spin-state shifts induced by the binding of the substrate in the active site of CYP106A1 were investigated using a double-beam spectrophotometer (UV-2101PC, Shimadzu, Japan) and two tandem quartz cuvettes. One chamber of each cuvette contained 10 μM CYP106A1 in 50 mM potassium phosphate buffer pH 7.4, while the other chamber was filled with buffer alone. The KBA acid dissolved in DMSO at a concentration of 5 mM was added into the P450 containing chamber of the sample cuvette. An equal amount of KBA was also added into the buffer containing chamber of the reference cuvette and spectral changes between 350 and 500 nm were recorded. The K_D value was determined by titrating the substrate KBA (0–220 μM final concentrations) until saturation. The data were analyzed by plotting the peak-to-trough differences (ΔA, 386–417 nm) against the substrate concentrations and the data fitting was done by sigmoidal regression using Origin software (OriginLab Corporation, Massachusetts, USA). All titrations were performed for three times, and the K_D value represents the mean of these three independent measurements.

In vitro conversion and kinetic analysis

The in vitro conversion of KBA was performed with a reconstituted system in a final volume of 250 μl at 30 °C for 30 min in 50 mM HEPES buffer containing 20 % glycerol. The reaction contained Arh1 (1.5 μM), Fdx/Fld (10 μM) and CYP106A1 (0.5 μM), a NADPH-regenerating system (1 mM $MgCl_2$, 5 mM glucose-6-phosphate, 1 U glucose-6-phosphate dehydrogenase) and 100 μM KBA. The reaction was started by the addition of NADPH in a final concentration of 1 mM. The reaction was stopped and extracted twice with 500 μl of ethyl acetate. The organic phases were combined, dried by solvent evaporation, resuspended in 200 μl methanol, and analyzed by high-performance liquid chromatography (HPLC). Assuming that the absorbance properties of the products are the same as those of the substrate, the overall product formation was calculated as the sum of the products compared to the sum of products and substrate. The values represent the mean of five independent reactions.

To determine kinetic parameters for the KBA conversion, the reactions were performed as mentioned above using 1.5 μM Arh1, 10 μM Fdx2, and 0.5 μM CYP106A1 for 2 min. The concentrations of KBA ranged from 0 to 100 μM. The V_{max} and K_M values were calculated by plotting the product formation rate against the substrate concentrations. The data fitting was done by hyperbolic regression using Origin software (OriginLab Corporation, Massachusetts, USA). The values represent the mean of four independent reactions.

HPLC analysis

HPLC analysis was performed using a Jasco system (Pu-980 HPLC pump, an AS-950 sampler, a UV-975 UV/visible detector, and a LG-980-02 gradient unit; Jasco, Gross-Umstadt, Germany). A reversed-phase ec MN Nucleodur C_{18} (3 μm, 4.0×125 mm) column (Macherey-Nagel, Bethlehem, PA, USA) was used for all experiments with a flow rate of 1 ml/min at a temperature of 40 °C. The mobile phase was methanol/water 75:25 (0.1 % TFA), and the detection wavelength was 254 nm.

Cytochrome *c* assay

To find out if a missing electron transfer between Arh1 and Fdx1 or between Fdx1 and CYP106A1 or both is the reason for the lack of conversion, we performed a cytochrome *c* assay. Therefore, cytochrome *c* (100 μM), Fdx1 (10 μM), and Arh1 (1 μM) were mixed in 500 μl 50 mM potassium phosphate buffer pH 7.4. The reaction was started by the addition of 200 μM NADPH, and the reduction of cytochrome *c* was monitored at 550 nm.

Whole-cell conversion using *B. megaterium* MS941

The *B. megaterium* strain MS941, a protease-deficient mutant of the *B. megaterium* strain DSM 319 (Wittchen and Meinhardt 1995), has been used for all whole-cell conversions. *B. megaterium* MS941 was transformed with the corresponding expression plasmids by the polyethylene glycol-mediated protoplast transformation method (Barg et al. 2005). All *B. megaterium* strains were cultivated in complex medium (consisting of 24 g/l yeast extract, 12 g/l soytone, 2.31 g/l KH_2PO_4, and 12.5 g/l K_2HPO_4) at 30 °C and 180 rpm in baffled flasks supplemented with 10 μg/ml tetracycline. For the whole-cell conversions, 50 ml of complex medium were inoculated with a single colony of *B. megaterium* and incubated overnight. Fifty milliliters of complex medium was inoculated with 500 μl of the overnight culture and further cultivated. When the OD_{578} reached 0.4, the protein expression was induced by the addition of 0.5 % (*w/v*) xylose. Twenty-four hours after induction, the cultures were harvested by centrifugation at 10,000×*g* for 15 min at 4 °C, resuspended in 25 ml 50 mM potassium phosphate buffer pH 7.4, and the substrate KBA dissolved in ethanol was added at a final concentration of 100 μM. Five hundred microliter samples of the cultures were taken after

defined time points. The extraction and HPLC analysis were performed as described above.

Large-scale conversion using *B. megaterium* MS941

To isolate the KBA products, the whole-cell conversions were scaled up to a volume of 750 ml. The incubation and induction were performed as described above. After 24 h of expression, the cultures were harvested by centrifugation, resuspended in 375 ml 50 mM potassium phosphate buffer pH 7.4, and KBA dissolved in ethanol was added in a final concentration of 100 μM. After 3 h the cultures were extracted twice with ethyl acetate. The organic phases were combined, dried by solvent evaporation, resuspended in methanol, and the products were purified from the extract by HPLC using a reversed-phase ec MN Nucleodur C_{18} (5 μm, 8.0×250 mm) column (Macherey-Nagel, Bethlehem, PA, USA).

NMR measurements

The NMR spectra were recorded in CD_3OD with a Bruker DRX 500 or a Bruker Avance 500 NMR spectrometer at 298 K. All chemical shifts were relative to CH_3OD at δ 3.30 (^{1}H NMR) or CD_3OD at δ 49.00 (^{13}C NMR) using the standard δ notation in parts per million. The 2D NMR spectra were recorded as gs-HH-COSY, gs-NOESY, gs-HSQCED, and gs-HMBC.

7β-hydroxy-11-keto-β-boswellic acid. ^{1}H NMR (500 MHz, CD_3OD, 298 K) δ5.53 (*s*, H-12), 4.01 (*dd*, *J*=11.0 and 4.5 Hz, H-7), 3.96 (*dd*, *J*=3.0 and 3.0 Hz, H-3), 2.46 (*s*, H-9), 2.33 (*ddd*, *J*=13.0, 4.0 and 4.0 Hz, H-1β), 2.18 (*m*, H-2β), 2.14 (*m*, H-15β), 2.13 (*m*, H-16α), 2.00 (*m*, H-6β), 1.84 (*m*, H-6α), 1.64 (*brd*, *J*=9.5 Hz, H-15α), 1.57 (*dd*, *J*=11.5 and 1.5 Hz, H-18), 1.51 (*m*, H-5), 1.50 (*m*, H-2α), 1.49 (*m*, H-19), 1.48 (*m*, H-22α), 1.43 (*m*, H-21β), 1.42 (*s*, 3H, H-27), 1.32 (*m*, 2H, H-21α and H-22β), 1.27 (*m*, H-1α), 1.26 (*s*, 3H, H-23), 1.14 (*s*, 3H, H-26), 1.11 (*s*, 3H, H-25), 0.99 (*m*, H-16β), 0.94 (*m*, H-20), 0.93 (*s*, 3H, H-30), 0.82 (*s*, 3H, H-28), 0.78 (*d*, *J*=6.5 Hz, 3H, H-29). ^{13}C NMR (125 MHz, CD_3OD, 298 K) δ 201.58 (*C*, C-11), 180.87 (*C*, C-24), 168.30 (*C*, C-13), 131.03 (*CH*, C-12), 73.61 (*CH*, C-7), 71.17 (*CH*, C-3), 61.94 (*CH*, C-9), 61.44 (*CH*, C-18), 51.51 (*C*, C-8), 47.94 (*C*, C-4), 46.66 (*C*, C-14), 46.40 (*CH*, C-5), 41.77 (CH_2, C-22), 40.69 (*CH*, C-19), 40.48 (*CH*, C-20), 38.54 (*C*, C-10), 35.02 (*C*, C-17), 34.63 (CH_2, C-1), 31.85 (CH_2, C-15), 31.82 (CH_2, C-21), 30.83 (CH_2, C-6), 29.32 (CH_3, C-28), 28.77 (CH_2, C-16), 26.81 (CH_2, C-2), 24.84 (CH_3, C-23), 21.34 (CH_3, C-30), 20.60 (CH_3, C-27), 17.75 (CH_3, C-29), 13.83 (CH_3, C-25), 12.26 (CH_3, C-26).

15α-hydroxy-11-keto-β-boswellic acid. Its ^{1}H and ^{13}C NMR data (500 and 125 MHz, CD_3OD, 298 K) were in good accordance with those from an authentic sample (Bleif et al. 2012).

7β,15α-dihydroxy-11-keto-β-boswellic acid. ^{1}H NMR (500 MHz, CD_3OD, 298 K) δ5.60 (*s*, H-12), 4.27 (*dd*, *J*=12.0 and 5.0 Hz, H-15), 4.01 (*dd*, *J*=11.5 and 5.0 Hz, H-7), 3.97 (*dd*, *J*=3.0 and 3.0 Hz, H-3), 2.44 (*s*, H-9), 2.37 (*ddd*, *J*=13.0, 4.0 and 4.0 Hz, H-1β), 2.23 (*dddd*, *J*=14.5, 14.5, 4.0 and 3.0 Hz, H-2β), 2.12 (*m*, H-16α), 2.04 (*dd*, *J*=13.5 and 11.5 Hz, H-6β), 1.94 (*ddd*, *J*=13.5, 5.0 and 2.0 Hz, H-6α), 1.60 (*dd*, *J*=11.5 and 1.5 Hz, H-18), 1.54 (*m*, 2H, H-5 and H-22α), 1.50 (*m*, H-2α), 1.48 (*m*, 2H, H-20 and H-21β), 1.37 (*s*, 3H, H-27), 1.36 (*m*, H-22β), 1.34 (*m*, H-21α), 1.31 (*m*, H-1α), 1.30 (*m*, H-16β), 1.28 (*s*, 3H, H-23), 1.18 (*s*, 3H, H-26), 1.14 (*s*, 3H, H-25), 0.97 (*m*, 4H, H-19 and H-30), 0.87 (*s*, 3H, H-28), 0.85 (*d*, *J*=6.5 Hz, 3H, H-29). ^{13}C NMR (125 MHz, CD_3OD, 298 K) δ 200.58 (*C*, C-11), 180.57 (*C*, C-24), 166.84 (*C*, C-13), 131.95 (*CH*, C-12), 72.60 (*CH*, C-7), 71.12 (*CH*, C-3), 67.71 (*CH*, C-15), 62.14 (*CH*, C-9), 61.49 (*CH*, C-18), 52.47 (*C*, C-14), 51.98 (*C*, C-8), 48.03 (*C*, C-4), 46.26 (*CH*, C-5), 41.53 (CH_2, C-22), 40.53 (*CH*, C-20), 40.43 (*CH*, C-19), 38.83 (*C*, C-10), 37.38 (CH_2, C-16), 35.08 (*C*, C-17), 34.62 (CH_2, C-1), 31.82 (CH_2, C-21), 30.01 (CH_3, C-28), 29.45 (CH_2, C-6), 28.06 (CH_2, C-2), 24.88 (CH_3, C-23), 21.35 (CH_3, C-30), 17.77 (CH_3, C-29), 14.89 (CH_3, C-27), 13.87 (CH_3, C-25), 12.60 (CH_3, C-26).

SDS-PAGE and Western Blot analysis

Aliquots of the *B. megaterium* cultures were adjusted to similar cell numbers, harvested by centrifugation and resuspended in 100 mM Tris/HCl buffer pH 8.0 containing 20 mM EDTA and 5 mg/ml lysozyme. The cell suspensions were incubated for 30 min at 37 °C and centrifuged at 15,000×*g* for 30 min to remove cell debris. The supernatant was mixed with an equal volume of 2× sodium dodecyl sulfate polyacrylamide gel electrophoresis (SDS-PAGE) loading buffer and the samples were separated on 15 % polyacrylamide gels (Laemmli 1970).

For Western Blot analysis of CYP106A1, Arh1, and Fld gels were blotted onto hybond-ECL nitrocellulose membranes, and the membranes were blocked overnight in Tris-buffered saline (TBS) buffer (50 mM Tris-base pH 7.5, 200 mM NaCl, 0.1 % Tween 20) containing 3 % milk powder. After washing three times with TBS buffer, the membranes were incubated with the primary antibody (1:1,000 dilution) in TBS buffer for 2 h. The primary antibodies against CYP106A1, Arh1, and Fld were produced by Charles River Company. The membranes were rinsed three times with TBS buffer and incubated with the secondary antibody (1:2,000 dilution), a horseradish peroxidase linked goat antirabbit IgG (Dako, Glostrup, Denmark) in TBS buffer for 1 h. After washing three times with phosphate-buffered saline (PBS) buffer (10 mM potassium phosphate buffer pH 7.4, 150 mM NaCl), the color development was started by adding 4 mg 4-chloro-1-naphtol (dissolved in 2 ml ethanol) and 10 μl 30 % H_2O_2 in 25 ml PBS buffer.

For Western Blot analysis of the ferredoxins, gels were blotted onto a polyvinylidene fluoride membrane, and the membrane was blocked for 15 min in PBS–Tween buffer (10 mM potassium phosphate buffer pH 7.4, 150 mM NaCl, 0.3 % Tween 20) containing 3 % milk powder. The membrane was incubated for 1 h with the anti-His_6 peroxidase (Roche Applied Science) in a 1:1,500 dilution. The membrane was washed three times with PBS–Tween buffer and the color development was started by adding 7.5 mg diaminobenzidine and 25 μl 30 % H_2O_2 in 30 ml PBS–Tween buffer.

Results

Bioinformatic analysis

Searching the *B. megaterium* DSM319 genome for genes encoding cytochromes P450, we identified genes encoding CYP106A1 (BM1), CYP102A1 (BM3), and two other cytochromes P450. We also identified one gene encoding a putative flavodoxin and four genes encoding putative ferredoxins (Fdx1-4) displaying candidate genes for potential natural redox partners of the cytochromes P450. Analysis of the protein domains using the Pfam Data base proved that Fdx1 contains a [2Fe–2S] cluster, while the other three ferredoxins were determined to belong to the [4Fe–4S] cluster ferredoxins. The flavodoxin and the ferredoxin genes are distributed over the whole genome, and none of them is located in the neighborhood of CYP106A1 (Fig. 1). Therefore, it was not possible to deduce the redox partners involved in the CYP106A1 system by the genomic context, and we decided to clone the cytochrome P450 CYP106A1 as well as the flavodoxin and the ferredoxins.

Expression, purification, and spectral characterization of the proteins

The cytochrome P450 CYP106A1, the flavodoxin Fld, and the four ferredoxins Fdx1, Fdx2, Fdx3, and Fdx4 were expressed in *E. coli* C43 (DE3) and purified by immobilized metal affinity chromatography and size exclusion chromatography. The purity of the heterologously expressed proteins was analyzed by SDS-PAGE (Fig. S1). The P450, Fld, and Fdx1 migrated at the expected sizes of 47.6, 16.5 and 11.7 kDa. Fdx2, Fdx3, and Fdx4 migrated between 15 and 25 kDa in contrast to the theoretical molecular weights of about 9 kDa indicating the formation of dimers.

The oxidized form of CYP106A1 displayed the typical peaks at 356, 417, 534, and 568 nm (Table 1) and the reduced and carbon monoxide bound form showed a characteristic peak at 450 nm with no indication of the inactive P420 form (Table 1 and Fig. 2a). The expression yield was 5,350 nmol-l^{-1} *E. coli* culture. The expression of Fld resulted in blue cell pellets as well as in a blue-gray lysate, which indicated that the protein was in the semiquinone form. During elution of Fld from the immobilized metal affinity chromatography column, the color turned to green and Fld maintained this color during size exclusion chromatography, concentration and storage. The pure protein showed maxima at 377 and 460 nm, a shoulder at 482 nm as well as a broad absorbance band from 550 to 650 nm characteristic for the semiquinone form (Table 1, Fig. 2b). Addition of potassium ferricyanide to Fld followed by concentration to remove the potassium ferricyanide from the Fld solution resulted in a loss of the absorbance at 550 to 650 nm indicating the oxidation of the flavin semiquinone to the fully oxidized quinone form (Table 1 and Fig. 2b). This quinone form was necessary to determine the molar extinction coefficient at the characteristic maximum of 460 nm, which was calculated to be 6,718 M^{-1} cm^{-1}. The expression yield was 5,733 nmol l^{-1} *E. coli* culture. Mixing of Fld and the reductase Arh1 from *S. pombe* did not alter the Fld semiquinone spectrum and was thus suitable to follow the reduction of the flavin chromophore. Addition of NADPH let to a decrease of the absorbance at 460 nm and an increase at 593 and 640 nm revealing the reduction of the flavin semiquinone to the hydroquinone form (Table 1 and Fig. 2b). Fdx1 was reddish-brown in color and displayed maxima at 317, 414, and 456 nm (Fig. 2c) characteristic for [2Fe–2S] cluster ferredoxins (Grinberg et al. 2000). The molar extinction coefficient was calculated as 4,283 M^{-1} cm^{-1}. The expression yield was 1,519 nmol l^{-1} *E. coli* culture (Table 1). Fdx2, Fdx3, and Fdx4 were green-brown colored and showed broad absorbance maxima from 390 to 400 nm (Table 1 and Fig. 2d) thus being non-[2Fe–2S] cluster ferredoxins, but [3Fe–4S] or [4Fe–4S] cluster ferredoxins (Sticht and Rösch 1998). The molar extinction coefficients were determined to be 6,671, 7,272, and 6,471 M^{-1} cm^{-1} for Fdx2, Fdx3, and Fdx4 (Table 1). The yields of the purified Fdx2, Fdx3, and Fdx4 were 3,052, 3,592, and 1,392 nmol l^{-1} *E. coli* culture (Table 1).

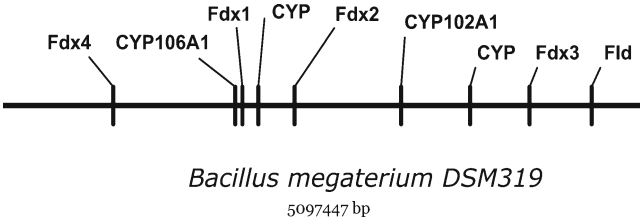

Fig. 1 Physical map of the *Bacillus megaterium* DSM319 chromosome and distribution of cytochrome P450, flavodoxin, and ferredoxin genes

Substrate binding spectrum

CYP106A2 from *B. megaterium* ATCC 13368 was recently described in our group to convert the pentacyclic triterpene

Table 1 Overview of the yield and the spectral characterization of the proteins from *B. megaterium* heterologously expressed in *E. coli*

Protein name	Yield [nmol l^{-1}]	Molar extinction coefficient [M^{-1} cm^{-1}]	UV-visible absorbance maximum (shoulder) [nm]
CYP106A1	5350	(Omura and Sato 1964)	ox: 356, 417, 534, 568
			red, CO bound: 450
Fld	5733	ε_{460}=6718	q: 377, 460, (482)
			sq: 377, 460, 550–650, (482)
			h: 593, 640
Fdx1	1519	ε_{414}=4283	317, 414, 456
Fdx2	3052	ε_{390}=6671	390
Fdx3	3592	ε_{390}=7272	390
Fdx4	1392	ε_{390}=6471	390

ox oxidized, *red* reduced form of CYP106A1, *q* quinone, *sq* semiquinone, *h* hydroquinone form of Fld

KBA (Bleif et al. 2012). As CYP106A1 shares a sequence identity of 63 % with CYP106A2, we tested if this substance can also be bound and converted by CYP106A1. Using difference spectroscopy, we first examined the ability of KBA to bind to the active site of CYP106A1. Binding of KBA to CYP106A1 induced a type I spectral shift characterized by a maximum at 386 nm and a minimum at 417 nm owing to the replacement of the axial water molecule by KBA. Titration of CYP106A1 with increasing amounts of KBA resulted in an equilibrium dissociation constant (K_D) of 92.25±2.98 μM and a Hill constant (n) of 1.46±0.02 (Fig. 3). The data followed a sigmoidal regression according to the Hill equation, which means that KBA shows a positive cooperative binding behavior towards CYP106A1.

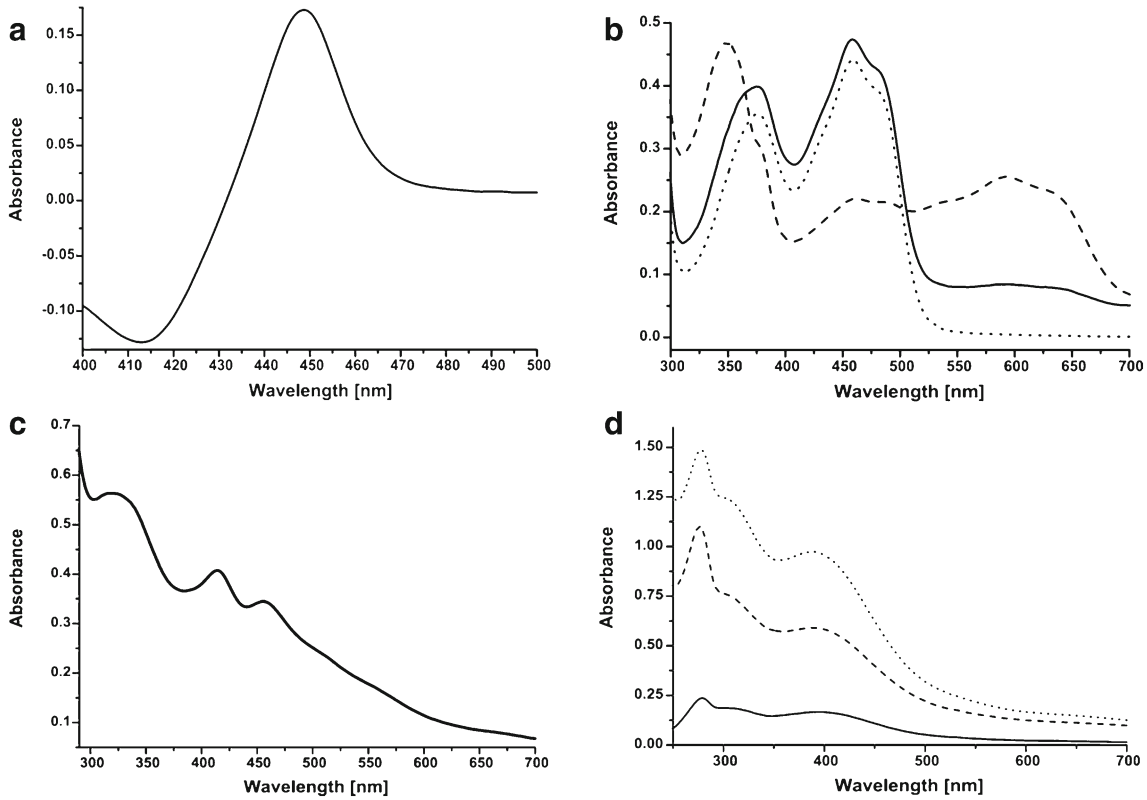

Fig. 2 UV–visible absorbance spectra of purified proteins. **a** After the reduction of CYP106A1 with sodium dithionite and purging with CO, the reduced CO complex was formed, which produced a typical peak at 450 nm. **b** Fld was purified in the semiquinone form (*solid line*) and could be reduced to the hydroquinone form (*dashed line*) and oxidized to the quinone form (*dotted line*). **c** Fdx1 displayed maxima at 317, 414, and 456 nm typical for [2Fe–2S] cluster ferredoxins. **d** The three [3Fe–4S] or [4Fe–4S] cluster ferredoxins, Fdx2 (*dotted line*), Fdx3 (*solid line*), and Fdx4 (*dashed line*) showed broad maxima at 390 to 400 nm characteristic for these type of ferredoxins

Reconstitution of CYP106A1 activity in vitro and kinetic analyses

As binding of a substance to the active site of a cytochrome is an obligatory, but not satisfactory prerequisite for substrate conversion, we next wanted to find out, if KBA can also be converted by CYP106A1. Generally, cytochromes P450 require electron transfer partners for their activity (Bernhardt 2006; Hannemann et al. 2007). We hence tested the ability of Fld and the ferredoxins to transfer electrons to CYP106A1. As no potential autologous reductase from *B. megaterium* DSM319 has been identified yet, we tested different heterologus reductases like Arh1 from fission yeast, bovine AdR, and *E. coli* Fpr concerning their ability to transfer electrons to Fld and the ferredoxins. Out of them, Arh1 showed the highest efficiency in transferring electrons to Fld and the ferredoxins (data not shown) and was therefore used for all further experiments. We found that Fld as well as the non-[2Fe–2S] cluster ferredoxins were able to support the CYP106A1 activity, whereas no activity could be observed using the [2Fe–2S] cluster ferredoxin Fdx1. To find out if a missing electron transfer between Arh1 and Fdx1 or between Fdx1 and the P450 or both is the reason for the lack of conversion, we performed a cytochrome *c* assay. As reduction of cytochrome *c* could be observed (data not shown), Fdx1 obviously is able to interact functionally with the reductase Arh1 and with cytochrome *c*, but not with CYP106A1 so that Fdx1 was not investigated further here. Using Fld, Fdx2, Fdx3, or Fdx4 together with Arh1 as redox partner, the pentacyclic triterpene KBA was converted by CYP106A1 to one main product P2 (~80 %) and one minor product P1 (~20 %) as depicted in Fig. 4. Thereby, the CYP106A1 dependent conversion of KBA showed another product pattern than observed for CYP106A2 (Bleif et al. 2012) indicating that the main product of the CYP106A1 dependent conversion of KBA is not 15α-hydroxy-KBA. As all of the four proteins led to the same product pattern, we compared their efficiency to act as electron mediator between Arh1 and CYP106A1. With 79.6±6.9 % and 79.3±6.4 % conversion in 30 min (Table 2), Fdx2 and Fdx3 showed almost the same product formation rates. In contrast, when using Fdx4 or Fld, only 60.6±3.3 or 27.2±2.6 % product formation in 30 min remained (Table 2). When the reaction was performed without redox partners as control, no product formation was observed (Table 2).

As Fdx2 showed the most efficient electron transfer between Arh1 and CYP106A1, Fdx2 was selected as redox partner to investigate the CYP106A1-dependent conversion of KBA by kinetic analyses. The catalytic activity of the KBA conversion showed a V_{max} of 5.4±0.1 nmol products per nmol CYP106A1 per minute and a K_M of 16.5±1.2 μM (Fig. 5).

Whole-cell conversions using *B. megaterium* MS941

After the successful conversion of KBA by CYP106A1 in vitro into one main and one minor product, our next aim was to provide sufficient amounts of the products to characterize them structurally by NMR spectroscopy. Recently, a xylose-inducible recombinant whole-cell system for the expression of cytochrome P450 systems in *B. megaterium* MS941 has been developed in our group (Bleif et al. 2012). We constructed recombinant whole-cell biocatalysts based on *B. megaterium* MS941 overexpressing only CYP106A1 (pSMF2.1B) or CYP106A1 together with the redox partners Arh1 and Fld (pSMF2.1BAFld), Fdx2 (pSMF2.1BAFdx2), Fdx3 (pSMF2.1BAFdx3), or Fdx4 (pSMF2.1BAFdx4). After protoplast transformation of *B.*

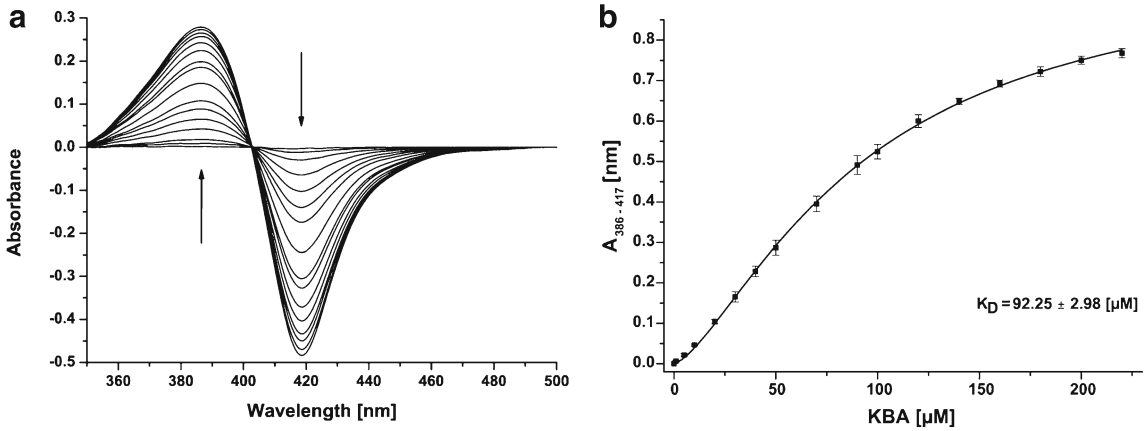

Fig. 3 **a** Type I spectral shift induced by the binding of KBA to CYP106A1. Increasing amounts of KBA dissolved in DMSO were titrated to CYP106A1 (10 μM in 50 mM potassium phosphate buffer pH 7.4). The final concentrations of KBA ranged from 0 to 220 μM. *Arrows* show the direction of the peak on increasing KBA concentrations. **b** The peak-to-trough absorbance differences were plotted against the corresponding concentrations of KBA titrated to CYP106A1. The mean values of the titrations were fitted by sigmoidal regression, and the K_D value was calculated to be 92.25±2.98 μM with a regression coefficient (R^2) of 0.99

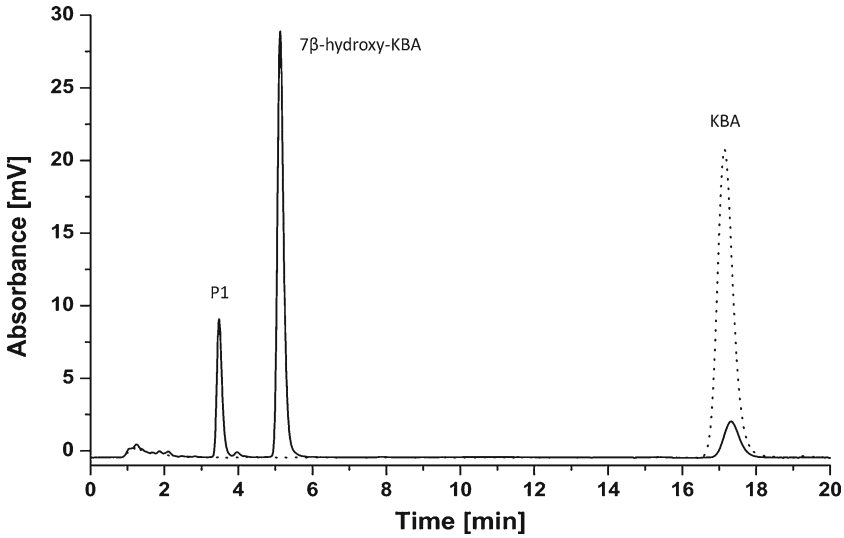

Fig. 4 HPLC chromatogram of the in vitro conversion of KBA by CYP106A1. The reaction was performed in 50 mM HEPES buffer containing 20 % glycerol at 30 °C for 30 min using 1.5 μM Arh1, 10 μM Fdx2, and 0.5 μM CYP106A1 (black line). KBA is converted to 7β-hydroxy-KBA and P1 (7β,15α-dihydroxy-KBA and 15α-hydroxy-KBA in a ratio 2:1). The negative control was conducted without CYP106A1 (*dotted line*)

megaterium with the corresponding plasmids and induction of the protein expression, Western blot analysis demonstrated the successful expression of all proteins (Fig. 6). The immunostaining showed that all proteins expressed in the whole-cell system arise at the same size as the purified proteins from *E. coli* (Fig. 6).

To investigate if the pentacyclic triterpene KBA can also be converted in vivo by the recombinant *B. megaterium* strains, the substrate KBA was added to the expression cultures 24 h after induction in a final concentration of 100 μM. After 3 h, samples of the cultures were taken, extracted, and analyzed by HPLC. The *B. megaterium* strains expressing only CYP106A1 or CYP106A1 together with the redox partners converted KBA to the same HPLC product pattern as observed in the in vitro assay using purified proteins (Figs. 7 and 4). The negative control, *B. megaterium* MS941 carrying the plasmid pSMF2.1, showed no conversion of KBA (Fig. 7).

NMR characterization of the bioconversion products

To provide sufficient amounts of the products for NMR spectroscopic analysis, a large-scale conversion of 100 μM KBA (18 mg) using *B. megaterium* MS941 overexpressing CYP106A1 (pSMF2.1B) was performed. Subsequent purification of the extract by HPLC led to two fractions P1 (4 mg) and P2 (12 mg), of which P2 was found to be a pure compound. In contrast to KBA, its ^{1}H and ^{13}C NMR data revealed an additional secondary hydroxyl group (δ_H. 4.01, *dd*; δ_C 73.61, *CH*), which could be located at C-7 by means of 2D NMR. Key correlations between H-7 (*dd*, J=11.0 and 4.5 Hz) and H-6α (δ_H 1.84, *m*) and H-6β (2.00, *m*) in the HHCOSY as well as between C-7 and H-5 (1.51, *m*), H-9 (2.46, *s*) and methyl H-26 (1.14, *s*, 3H) in the HMBC resolved all doubt. The stereochemistry at C-7 could immediately be deduced from the coupling pattern of H-7 ($J_{ax/ax}$=11.0 and $J_{ax/eq}$ 4.5 Hz) with H-6α and H-6β, indicating an axial position

Table 2 Comparison of the conversion of 100 μM KBA by CYP106A1 in reconstituted in vitro systems and in whole-cell biocatalysts

Percent conversion			
In vitro system[a]		Whole-cell biocatalysts[b]	
		pSMF2.1	0
CYP106A1	0	pSMF2.1B	53.3±5.9
Arh1+Fld+CYP106A1	27.2±2.6	pSMF2.1BAFld	88.1±8.7
Arh1+Fdx2+CYP106A1	79.6±6.9	pSMF2.1BAFdx2	96.5±4.1
Arh1+Fdx3+CYP106A1	79.3±6.4	pSMF2.1BAFdx3	83.6±10.4
Arh1+Fdx4+CYP106A1	60.6±3.3	pSMF2.1BAFdx4	98.8±0.2

[a] In vitro conversion of 100 μM KBA within 30 min using no redox partners or Arh1 together with Fld, Fdx2, Fdx3, or Fdx4

[b] In vivo conversion of 100 μM KBA within 100 min using different *B. megaterium* strains expressing only CYP106A1 or CYP106A1 and Arh1 together with Fld, Fdx2, Fdx3, or Fdx4

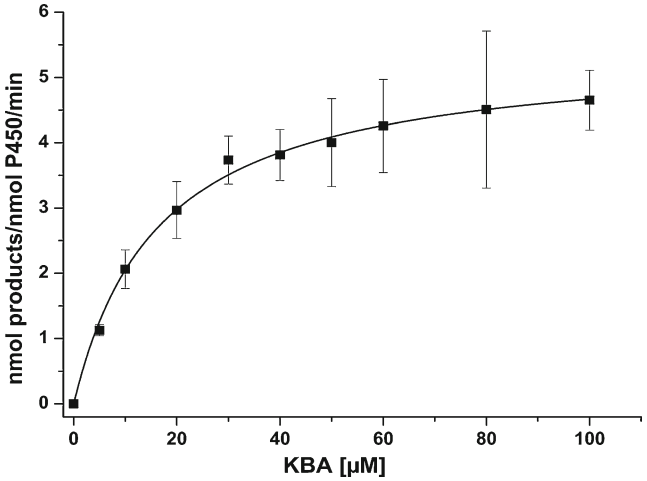

Fig. 5 Determination of kinetic parameters for the KBA conversion catalyzed by CYP106A1. The reactions were performed in 50 mM HEPES buffer containing 20 % glycerol at 30 °C for 2 min using 1.5 μM Arh1, 10 μM Fdx2, and 0.5 μM CYP106A1. The concentrations of KBA ranged from 0 to 100 μM

of the therefore α-oriented H-7. All considerations for P2 led to the structure of *7β-hydroxy-11-keto-β-boswellic acid*.

P1 was found to be a 2:1 mixture (Scheme 1) of two similar compounds, of which the minor one could be recognized as *15α-hydroxy-11-keto-β-boswellic acid*, recently described by our group for the first time (Bleif et al. 2012). NMR investigation of the major compound led to a dihydroxylated product. Its ^{1}H and ^{13}C NMR data showed great similarities to *7β*- and *15α*-KBA, and therefore, its structure was supposed to be *7β,15α*-dihydroxy-11-keto-β-boswellic acid, which could be elucidated by means of 2D NMR, including HHCOSY, HSQCED, HMBC and NOESY. The synthesis and NMR analysis of 7β-hydroxy-KBA and 7β,15α-dihydroxy-KBA have not been described in the literature yet.

Time-dependent conversion of KBA

To examine if the *B. megaterium* MS941 strains constructed in this study show differences in the KBA product formation in dependence on the redox partners, we performed time-dependent in vivo conversions with these five strains expressing CYP106A1 (pSMF2.1B) or expressing CYP106A1, Arh1, and Fld (pSMF2.1BAFld), Fdx2 (pSMF2.1BAFdx2), Fdx3 (pSMF2.1BAFdx3), or Fdx4 (pSMF2.1BAFdx4). The substrate KBA was added to the expression cultures 24 h after induction in a final concentration of 100 μM, and samples were taken after 0, 10, 20, 40, 60, 80, and 100 min (Fig. 8). The strain expressing only CYP106A1 showed the lowest product formation over the whole time period (Fig. 8); after 100 min only 53.3±5.9 % conversion was achieved (Table 2). In contrast, by overexpressing the redox partners, the product formation was enhanced: After 100 min, 88.1±8.7 % and 83.6±10.4 % product formation were observed expressing Fld or Fdx3 and Arh1 additionally to CYP106A1 (Fig. 8, Table 2). Using Fdx2 or Fdx4 as redox partner, even 96.5±4.1 % and 98.8±0.2 % product formation were found (Fig. 8). The negative control, *B. megaterium* MS941 carrying the plasmid pSMF2.1, showed no conversion of KBA within this time period (Table 2). During the complete time period, the strains additionally expressing the redox partners showed a better conversion than the strain only expressing CYP106A1 with Fdx4 being slightly faster than Fdx2, followed by Fld and Fdx3 (Fig. 8).

Discussion

Cytochromes P450 are versatile biocatalysts that catalyze the regio-, chemo-, and stereospecific oxidation of diverse substrates and are therefore important candidates for biotechnological applications (Bernhardt 2006). Thereby, new sequencing projects enable the discovery and characterization of new cytochromes P450 with novel substrate spectra, selectivities and reaction mechanisms. Recently, the genome of the *B. megaterium* strain DSM319 has been sequenced (Eppinger et al. 2011) to fully exploit the potential of this industrially important organism. In the genome of *B. megaterium* DSM319 (Wittchen and Meinhardt 1995), we identified a gene encoding the cytochrome P450 CYP106A1 (BM1), whose closest homologue, CYP106A2 from *B. megaterium* ATCC 13368, has recently been described in our group to bind and to convert the pentacyclic triterpene KBA (Bleif et al. 2012). Like with CYP106A2, KBA also induced a type I shift with CYP106A1 (Fig. 3). With 92.25±2.98 μM the equilibrium dissociation constant (K_D) was almost three times higher than in the case of CYP106A2 (K_D 33.34±2.87 μM) (Bleif et al. 2012) indicating a weaker binding of KBA to CYP106A1 than to CYP106A2. Differences in the binding are also reflected by the fact that the data followed a hyperbolic regression for CYP106A2 and a sigmoidal regression according to the Hill equation for CYP106A1 suggestive for cooperativity at the level of ligand binding or at the level of spin-state conversion (Lampe et al. 2008). After we demonstrated that CYP106A1 can bind KBA, we next wanted to identify redox partners for CYP106A1. The homologous redox partners of the close homologue CYP106A2—a NADPH-dependent flavoprotein (megaredoxin reductase) and an iron-sulfur protein (megaredoxin)—have been purified (Berg et al. 1976), but never cloned and the genome of *B. megaterium* ATCC 13368 has not been sequenced so far. As, in contrast to *B. megaterium* ATCC 13368, the genome of *B. megaterium* DSM319 has been sequenced (Eppinger et al. 2011), we, therefore, also aimed for identifying the natural redox partners of CYP106A1. One way to identify potential redox partners of P450s is to study neighboring genes of the respective P450. Unfortunately, CYP106A1 is found without any associated genes encoding electron transfer proteins such as ferredoxins and flavodoxins (Fig. 1) immediately upstream or downstream,

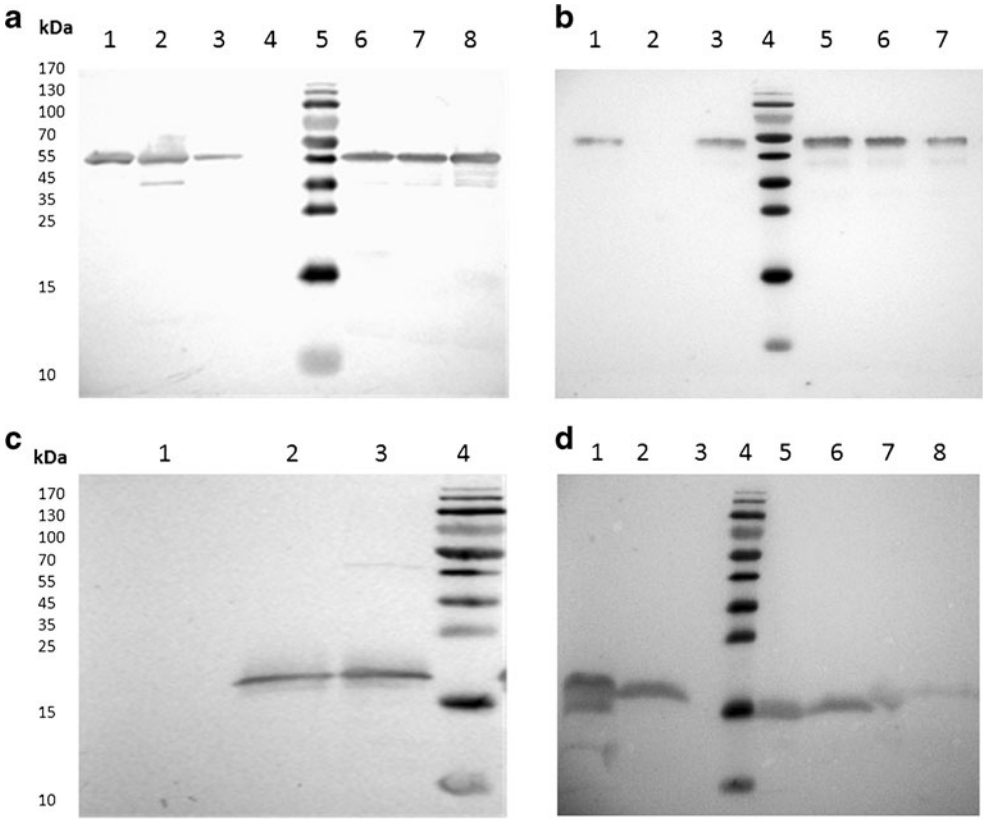

Fig. 6 Western blot analysis performed with polyclonal antibodies directed against CYP106A1 (**a**), Arh1 (**b**), Fld (**c**), and a monoclonal antibody directed against His_6 (**d**). **a** *Lane 1* shows the purified protein CYP106A1, *lanes 2–4* the lysates of the *B. megaterium* strains containing pSMF2.1B (*lane 2*), pSMF2.1BAFld (*lane 3*), and pSMF2.1 (*lane 4*) 24 h after induction. *Lane 5* contains the prestained molecular weight marker. *Lanes 6–8* represent lysates of the *B. megaterium* strains containing pSMF2.1BAFdx2, pSMF2.1BAFdx3, and pSMF2.1BAFdx4 24 h after induction. **b** The purified protein Arh1 is shown in *lane 1*. *Lane 2* represents the lysate of the *B. megaterium* strain containing pSMF2.1 24 h after induction. In *lane 3*, a sample of the lysate of the *B. megaterium* strain comprising pSMF2.1BAFld 24 h after induction was applied. *Lane 4* shows the prestained molecular weight marker. *Lanes 5–7* represent samples of lysates of the *B. megaterium* strains containing pSMF2.1BAFdx2, pSMF2.1BAFdx3, and pSMF2.1BAFdx4 24 h after induction. **c** *Lane 1* represents the lysate of the *B. megaterium* strain containing pSMF2.1 24 h after induction, *lane 2* the purified protein Fld, *lane 3* the lysate of the *B. megaterium* strain containing pSMF2.1BAFld 24 h after induction, and *lane 4* the prestained molecular weight marker. **d** The purified proteins Fdx2, Fdx3, and Fdx4 are shown in the *lanes 1*, *5*, and *7*. *Lanes 2*, *3*, *6*, and *8* represent samples of lysates of the *B. megaterium* strains containing pSMF2.1BAFdx2, pSMF2.1, pSMF2.1BAFdx3, and pSMF2.1BAFdx4 24 h after induction. The prestained molecular weight marker was applied to *lane 4*

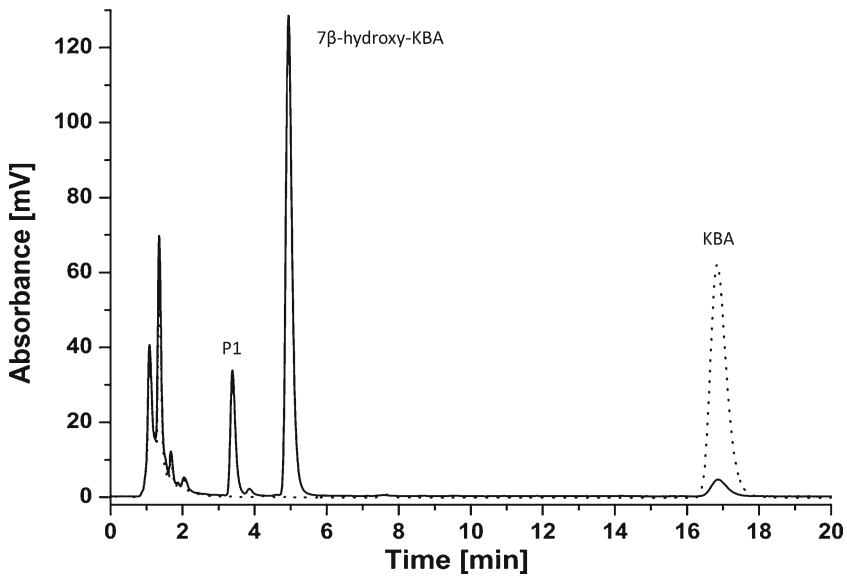

Fig. 7 HPLC chromatograms of the in vivo conversion of KBA using recombinant *B. megaterium* MS941 strains. *B. megaterium* MS941 containing the plasmid pSMF2.1B (*solid line*) converted KBA to 7β-hydroxy-KBA and P1 (7β,15α-dihydroxy-KBA and 15α-hydroxy-KBA in a ratio 2:1). The negative control *B. megaterium* MS941 carrying the plasmid pSMF2.1 (*dotted line*) showed no conversion of KBA. The reactions were performed in 25 ml potassium phosphate buffer pH 7.4 at 30 °C for 3 h with 100 μM KBA

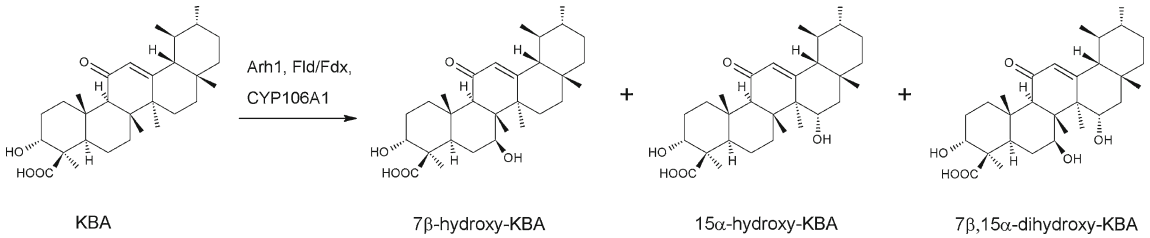

Scheme 1 Hydroxylation of KBA catalyzed by the CYP106A1 system

like already observed for other P450s (Bell et al. 2006; Ewen et al. 2009). We, therefore, decided to search for potential natural electron transfer proteins in the complete genome of *B. megaterium* DSM319 by their sequence identity to known electron transfer proteins. We identified a gene encoding a flavodoxin as well as a gene encoding a [2Fe–2S] cluster ferredoxin and three genes encoding [3Fe–4S] or [4Fe–4S] cluster ferredoxins. These proteins contribute to the great variety of possible electron transfer systems of the P450s (Hannemann et al. 2007). We succeeded in overexpressing all these genes in *E. coli* and in purifying them to homogeneity. Next, we tested if Fld and the ferredoxins are capable to functionally interact with CYP106A1 by investigating their ability to support the CYP106A1-dependent conversion of the pentacyclic triterpene KBA. We found that KBA was successfully converted by CYP106A1 to one main and one minor product. Thereby, Fld as well as the non-[2Fe–2S] cluster ferredoxins Fdx2, Fdx3, and Fdx4 were able to support the CYP106A1 activity by interacting with the heterologous reductase Arh1 from *S. pombe*. To our surprise, the [2Fe–2S] cluster ferredoxin Fdx1 failed to deliver electrons to CYP106A1 (Scheme 2). According to these results, Fld, Fdx2, Fdx3, and Fdx4 can be considered as potential natural redox partners of CYP106A1 in *B. megaterium* DSM 319 as summarized in Scheme 2. Non-[2Fe–2S] cluster ferredoxins have been reported to interact with cytochromes P450: CYP107H1 from *B. subtilis* (Green et al. 2003), the P450mor system from *Mycobacterium* sp. strain HE5 (Sielaff and Andreesen 2005), the CYP51 system from *M. tuberculosis* (McLean et al. 2006), the CYP105D system from *Streptomyces coelicolor* (Chun et al. 2007) and the CYP260A1 system from *Sorangium cellulosum* So ce56 (Ewen et al. 2009) are examples for non-[2Fe–2S] cluster ferredoxins as redox partners of bacterial cytochromes P450. There are also several examples known for flavodoxins being able to act as electron transfer proteins in cytochrome P450 systems. Flavodoxin reductase and flavodoxin from *E. coli* are capable to substitute for the endogenous redox partners of some heterologously expressed cytochromes P450 (Barnes et al. 1991; Jenkins and Waterman 1994). The flavodoxin *An*Fld from the cyanobacterium *Anabaena* PCC 7119 is able to interact with CYP106A2 from *B. megaterium* ATCC 13368 (Goni et al. 2009). With the flavodoxin cindoxin from *Citrobacter brakii* as redox partner for CYP176A1 (P450cin) the first cytochrome P450 system containing a flavodoxin as physiological redox protein was discovered (Hawkes et al. 2002). Recently, two flavodoxins from *Clostridium acetobutylicum* acting as potential electron transfer partners for CYP152A2 were found (Malca et al. 2011). The *Bacillus subtilis* flavodoxins YkuN and YkuP can also serve as redox partners for CYP107H1 (Lawson et al. 2004) and CYP109B1 (Girhard et al. 2010) from *B. subtilis*. Interestingly, these two P450s can interact with ferredoxins as well: The activity of CYP109B1 can be reconstituted with different heterologous [2Fe–2S] cluster ferredoxins (Girhard et al. 2010) and, as mentioned above, the [4Fe–4S] cluster ferredoxin Fer is capable of transferring electrons to CYP107H1, albeit at a very low rate (Green et al. 2003). Here, we report the discovery of a cytochrome P450 that is able to accept electrons from a flavodoxin and from non-[2Fe–2S] cluster ferredoxins. But in contrast to the CYP107H1 system, in this study, Fld and the ferredoxins support the CYP106A1 activity very efficiently.

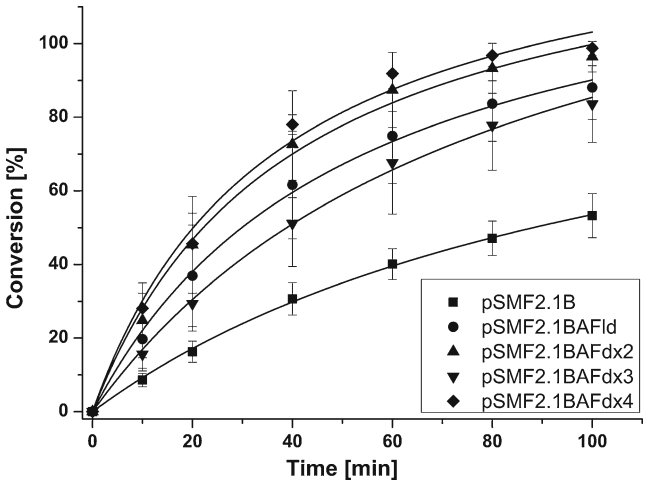

Fig. 8 Conversion of KBA by different *B. megaterium* MS941 strains expressing CYP106A1 (*squares*, pSMF2.1B) or expressing CYP106A1, Arh1, and Fld (*circles*, pSMF2.1BAFld), Fdx2 (*triangles bottom*, pSMF2.1BAFdx2), Fdx3 (*triangles top*, pSMF2.1BAFdx3) or Fdx4 (*diamonds*, pSMF2.1BAFdx4). The reactions were performed in 25 ml potassium phosphate buffer pH 7.4 at 30 °C with 100 μM KBA and samples were taken after 0, 10, 20, 40, 60, 80, and 100 min

To examine the electron transfer in this cytochrome P450 system in more detail, we compared the four redox partners concerning their efficiency to act as electron mediator between Arh1 and CYP106A1. In the HPLC-based in vitro KBA conversion assay Fdx2 and Fdx3 showed the highest product

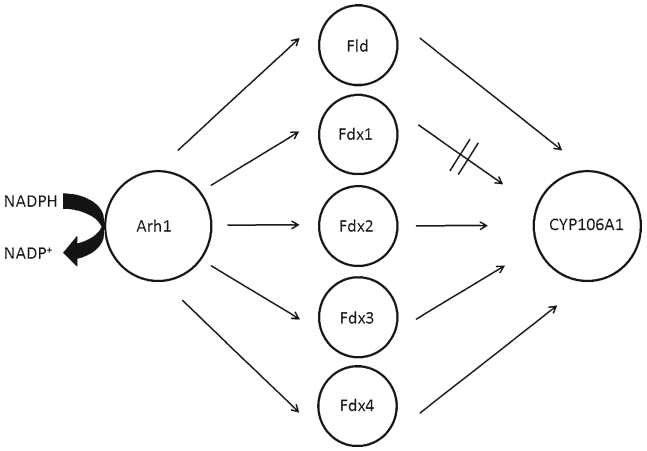

Scheme 2 Overview of the novel P450 system discovered in this work consisting of Arh1 from *S. pombe* as well as flavodoxin or one of three [3Fe–4S] or [4Fe–4S] cluster ferredoxins and CYP106A1 from *B. megaterium* DSM319

formation rates, while the activity was lower when using Fdx4 or Fld. In addition to the in vitro reactions, we also compared the different redox partners in vivo. We therefore constructed whole-cell biocatalysts based on *B. megaterium* MS941 overexpressing CYP106A1, the reductase Arh1 and either Fld, Fdx2, Fdx3, or Fdx4. Additionally, we constructed a *B. megaterium* MS941 strain overexpressing only CYP106A1 without redox partners. The latter strain already showed a quite efficient in vivo conversion of KBA, indicating the presence and activity of electron transfer proteins from *B. megaterium* MS941. Nevertheless, by overexpressing the redox partners in addition to the P450, the product formation was significantly increased revealing that the concentrations of the redox proteins are the limiting parameters in this whole-cell system. The fact that the individual redox partners showed different product formation rates in vitro and in vivo might be explained by different expression levels and stabilities of the redox proteins or by different ratios between the proteins: While in vitro a ratio of 3:20:1 was used for Arh1:Fld/Fdx:CYP106A1, the ratio in vivo was 1:1:1 according to the cloning of the genes into a tricistronic vector and subsequent translation of the proteins in equal amounts.

To investigate the CYP106A1-dependent conversion of KBA in more detail, we performed in vitro kinetic analyses and calculated a V_{max} of 5.4±0.1 nmol products/nmol CYP106A1/min and a K_M of 16.5±1.2 μM. The data here followed a hyperbolic regression although a sigmoidal binding of KBA had been observed analyzing the type I spin shift. Acccording to this data, CYP106A1 shows a lower rate of the KBA conversion in comparison with CYP106A2 (V_{max} of 97.4 nmol products/nmol CYP106A2/min). A sigmoidal regression concerning the substrate binding and a hyperbolic regression concerning kinetic analysis was also observed in the case of CYP3A4 and Nile Red as substrate (Lampe et al. 2008). In this study, the authors suggest that the first Nile Red and subsequent Nile Red molecules differentially disturb the heme spin state but do not yield CYP complexes with different kinetic parameters, at least within the resolution of their assay (Lampe et al. 2008). This explanation could also be appropriate for CYP106A1 and the substrate KBA, but further experiments are necessary in order to elucidate the detailed mechanisms.

Using the CYP106A1 system, we were able to convert the pentacyclic triterpene KBA in vitro and in vivo into one main and one minor product, whereby the CYP106A1-dependent conversion showed another product pattern than that observed for CYP106A2 (Bleif et al. 2012). Therefore, our next aim was to provide sufficient amounts of the products of the CYP106A1 dependent KBA conversion to characterize them structurally by NMR spectroscopy. The two products were identified as 7β-hydroxy-KBA for the main product and a mixture of 7β,15α-dihydroxy-KBA and 15α-hydroxy-KBA in a ratio of 2:1 for the minor product. 15α-Hydroxy-KBA could also be identified as the main product of the CYP106A2-dependent conversion of KBA (Bleif et al. 2012), whereas the synthesis and NMR analysis of 7β-hydroxy-KBA and 7β,15α-dihydroxy-KBA have not been described in the literature yet. Pentacyclic triterpenes (PTs) possess a wide range of unique biological activities and exhibit clinical significance as multitarget therapeutic agents for the prevention and treatment of metabolic and vascular diseases (Sheng and Sun 2011). Boswellic acids (BAs), the main bioactive constituents of *B. serrata* gum resin extracts, are used in Indian ayurvedic medicine to treat inflammatory disorders and arthritic diseases (Krüger et al. 2008; Gupta et al. 2001). The molecular targets of the pharmacological actions of BAs are 5- and 12-lipoxygenase (Poeckel and Werz 2006), cyclooxygenase-1 (Siemoneit et al. 2008), human leukocyte elastase (Safayhi et al. 1997), the nuclear factor-KB (Syrovets et al. 2005), topoisomerases (Syrovets et al. 2000), cathepsin G (Tausch et al. 2009), and the microsomal prostaglandin E2 synthase (Werz et al. 2009). However, pharmacokinetic studies revealed poor bioavailability, especially of KBA, one of the most potent BAs (Krüger et al. 2008), which could potentially be enhanced by structural modifications of KBA like the hydroxylation of carbon atoms. The hydroxylation of non-activated carbon atoms like the C7 of KBA represents a reaction that is not possible by standard chemical means (Rabe et al. 2008). The novel substances identified in this study are, therefore, interesting KBA derivatives that can possibly show an enhanced bioavailability or improved pharmaceutical activities compared to the substrate KBA or can be the basis for additional modifications by chemical methods. Thus, using a *B. megaterium* whole-cell system overexpressing CYP106A1, we were able to efficiently convert KBA to the same product pattern as observed in vitro using purified proteins. The additional overexpression of the redox partners in vivo increased the productivity 1.5- to almost 2-fold. The CYP106A1 whole-

cell system is able to completely convert KBA within 100 min with 80 % selectivity for the main-product, shown to be 7β-hydroxy-KBA. With a calculated yield of 560.7 mg 7β-hydroxy-KBA/l/d the CYP106A1 system exhibits the same productivity as observed for the 15α-hydroxy-KBA production by the CYP106A2 system (Bleif et al. 2012).

Altogether, we identified a new cytochrome P450 system and four potential autologous redox chains from *B. megaterium* that were successfully applied in whole-cell systems for the production of the novel substance 7β-hydroxy-KBA as well as a mixture of 15α-hydroxy-KBA and 7β,15α-dihydroxy-KBA, which can be the basis for applying methods of synthetic biology to introduce additional modifications into this complex molecule for the production of more efficient drugs.

Acknowledgments The authors thank Prof. Dr. Dieter Jahn (TU Braunschweig) for the kind provision of the *B. megaterium* strain MS941 and Dr. Rebekka Biedendieck (TU Braunschweig) for constructive discussions.

References

Barg H, Malten M, Jahn M, Jahn D (2005) Protein and vitamin production in *Bacillus megaterium*, vol 18. Microbial processes and products, 1st edn. Humana, Totowa, pp 205–223

Barnes HJ, Arlotto MP, Waterman MR (1991) Expression and enzymatic activity of recombinant cytochrome P450 17 alpha-hydroxylase in *Escherichia coli*. Proc Natl Acad Sci USA 88:5597–5601

Bell SG, Hoskins N, Xu F, Caprotti D, Rao Z, Wong LL (2006) Cytochrome P450 enzymes from the metabolically diverse bacterium *Rhodopseudomonas palustris*. Biochem Biophys Res Commun 342:191–196

Berg A, Gustafsson JA, Ingelman-Sundberg M (1976) Characterization of a cytochrome P-450-dependent steroid hydroxylase system present in *Bacillus megaterium*. J Biol Chem 251:2831–2838

Berg A, Ingelman-Sundberg M, Gustafsson JA (1979) Isolation and characterization of cytochrome P-450meg. Acta Biol Med Ger 38:333–344

Bernhardt R (1996) Cytochrome P450: structure, function, and generation of reactive oxygen species. Rev Physiol Biochem Pharmacol 127:137–221

Bernhardt R (2006) Cytochromes P450 as versatile biocatalysts. J Biotechnol 124:128–145

Bernhardt R, Waterman M (2007) Cytochrome P450 and steroid hormone biosynthesis. In: Sigel A, Sigel H, Sigel RKO (eds) The ubiquitous roles of cytochrome P450 proteins. Wiley, New York, pp 361–396

Bleif S, Hannemann F, Zapp J, Hartmann D, Jauch J, Bernhardt R (2012) A new *Bacillus megaterium* whole-cell catalyst for the hydroxylation of the pentacyclic triterpene 11-keto-beta-boswellic acid (KBA) based on a recombinant cytochrome P450 system. Appl Microbiol Biotechnol 93:1135–1146

Chun Y, Shimada T, Sanchez-Ponce R, Martin MV, Lei L, Zhao B, Kelly SL, Waterman MR, Lamb DC, Guengerich FP (2007) Electron transport pathway for a *Streptomyces* cytochrome P450: cytochrome P450 105D5-catalyzed fatty acid hydroxylation in *Streptomyces coelicolor* A3(2). J Biol Chem 282:17486–17500

Eppinger M, Bunk B, Johns MA, Edirisinghe JN, Kutumbaka KK, Koenig SSK, Creasy HH, Rosovitz MJ, Riley DR, Daugherty S, Martin M, Elbourne LDH, Paulsen I, Biedendieck R, Braun C, Grayburn S, Dhingra S, Lukyanchuk V, Ball B, Ul-Qamar R, Seibel J, Bremer E, Jahn D, Ravel J, Vary PS (2011) Genome sequences of the biotechnologically important *Bacillus megaterium* strains QM B1551 and DSM319. J Bacteriol 193:4199–4213

Ewen KM, Schiffler B, Takasaki Y, Bernhardt R, Hannemann F (2008) The endogenous adrenodoxin reductase-like flavoprotein arh1 supports heterologous cytochrome P450-dependent substrate conversions in *Schizosaccharomyces pombe*. FEMS Yeast Res 8:432–441

Ewen KM, Hannemann F, Khatri Y, Perlova O, Kappl R, Krug D, Hüttermann J, Müller R, Bernhardt R (2009) Genome mining in *Sorangium cellulosum* So ce56: identification and characterization of the homologous electron transfer proteins of a myxobacterial cytochrome P450. J Biol Chem 284:28590–28598

Finn RD, Mistry J, Tate J, Coggill P, Heger A, Pollington JE, Gavin OL, Gunasekaran P, Ceric G, Forslund K, Holm L, Sonnhammer ELL, Eddy SR, Bateman A (2010) The Pfam protein families database. Nucleic Acids Res 38:D211–D222

Freigang J, Diederichs K, Schäfer KP, Welte W, Paul R (2002) Crystal structure of oxidized flavodoxin, an essential protein in *Helicobacter pylori*. Protein Sci 11:253–261

Girhard M, Klaus T, Khatri Y, Bernhardt R, Urlacher VB (2010) Characterization of the versatile monooxygenase CYP109B1 from *Bacillus subtilis*. Appl Microbiol Biotechnol 82:595–607

Goni G, Zöllner A, Lisurek M, Velazquez-Campoy A, Pinto S, Gomez-Moreno C, Hannemann F, Bernhardt R, Medina M (2009) Cyanobacterial electron carrier proteins as electron donors to CYP106A2 from *Bacillus megaterium* ATCC 13368. Biochim Biophys Acta 1794:1635–1642

Green AJ, Munro AW, Cheesman MR, Reid GA, von Wachenfeldt C, Chapman SK (2003) Expression, purification and characterisation of a *Bacillus subtilis* ferredoxin: a potential electron transfer donor to cytochrome P450 BioI. J Inorg Biochem 93:92–99

Grinberg AV, Hannemann F, Schiffler B, Müller J, Heinemann U, Bernhardt R (2000) Adrenodoxin: structure, stability, and electron transfer properties. Proteins 40:590–612

Gupta I, Parihar A, Malhotra P, Gupta S, Ludtke R, Safayhi H, Ammon HP (2001) Effects of gum resin of *Boswellia serrata* in patients with chronic colitis. Planta Med 67:391–395

Hannemann F, Bichet A, Ewen KM, Bernhardt R (2007) Cytochrome P450 systems-biological variations of electron transport chains. Biochim Biophys Acta 1770:330–344

Hawkes DB, Adams GW, Burlingame AL, Ortiz de Montellano PR, De Voss JJ (2002) Cytochrome P450(cin) (CYP176A), isolation, expression, and characterization. J Biol Chem 277:27725–27732

He JS, Fulco AJ (1991) A barbiturate-regulated protein binding to a common sequence in the cytochrome P450 genes of rodents and bacteria. J Biol Chem 266:7864–7869

Jauch J, Bergmann J (2003) An efficient method for the large-scale preparation of 3-O-acetyl-11-oxo-β-boswellic acid and other boswellic acids. Eur J Org Chem 2003:4752–4756

Jenkins CM, Waterman MR (1994) Flavodoxin and NADPH-flavodoxin reductase from *Escherichia coli* support bovine cytochrome P450c17 hydroxylase activities. J Biol Chem 269:27401–27408

Khatri Y, Hannemann F, Ewen KM, Pistorius D, Perlova O, Kagawa N, Brachmann AO, Müller R, Bernhardt R (2010) The CYPome of *Sorangium cellulosum* So ce56 and identification of CYP109D1 as a new fatty acid hydroxylase. Chem Biol 17:1295–1305

Knight E Jr, D'Eustachio AJ, Hardy RW (1966) Flavodoxin: a flavoprotein with ferredoxin activity from *Clostrium pasteurianum*. Biochim Biophys Acta 113:626–628

Krüger P, Daneshfar R, Eckert GP, Klein J, Volmer DA, Bahr U, Müller WE, Karas M, Schubert-Zsilavecz M, Abdel-Tawab M (2008) Metabolism of boswellic acids *in vitro* and *in vivo*. Drug Metab Dispos 36:1135–1142

Laemmli UK (1970) Cleavage of structural proteins during the assembly of the head of bacteriophage T4. Nature 227:680–685

Lampe JN, Fernandez C, Nath A, Atkins WM (2008) Nile Red is a fluorescent allosteric substrate of cytochrome P450 3A4. Biochemistry 47:509–516

Lawson RJ, von Wachenfeldt C, Haq I, Perkins J, Munro AW (2004) Expression and characterization of the two flavodoxin proteins of *Bacillus subtilis*, YkuN and YkuP: biophysical properties and interactions with cytochrome P450 BioI. Biochemistry 43:12390–12409

Malca SH, Girhard M, Schuster S, Dürre P, Urlacher VB (2011) Expression, purification and characterization of two *Clostridium acetobutylicum* flavodoxins: potential electron transfer partners for CYP152A2. Biochim Biophys Acta 1814:257–264

Malten M, Hollmann R, Deckwer WD, Jahn D (2005) Production and secretion of recombinant *Leuconostoc mesenteroides* dextransucrase DsrS in *Bacillus megaterium*. Biotechnol Bioeng 89:206–218

McLean KJ, Warman AJ, Seward HE, Marshall KR, Girvan HM, Cheesman MR, Waterman MR, Munro AW (2006) Biophysical characterization of the sterol demethylase P450 from *Mycobacterium tuberculosis*, its cognate ferredoxin, and their interactions. Biochemistry 45:8427–8443

Meinhardt F, Stahl U, Ebeling W (1989) Highly efficient expression of homologous and heterologous genes in *Bacillus megaterium*. Appl Microbiol Biotechnol 30:343–350

Nguyen KT, Virus C, Günnewich N, Hannemann F, Bernhardt R (2012) Changing the regioselectivity of a P450 from C15 to C11 hydroxylation of progesterone. ChemBioChem 13:1161–1166

Omura T, Sato R (1964) The carbon monoxide-binding pigment of liver microsomes. I. Evidence for its hemoprotein nature. J Biol Chem 239:2370–2378

Poeckel D, Werz O (2006) Boswellic acids: biological actions and molecular targets. Curr Med Chem 13:3359–3369

Puan K, Wang H, Dairi T, Kuzuyama T, Morita CT (2005) fldA is an essential gene required in the 2-C-methyl-D-erythritol 4-phosphate pathway for isoprenoid biosynthesis. FEBS Lett 579:3802–3806

Rabe KS, Gandubert VJ, Spengler M, Erkelenz M, Niemeyer CM (2008) Engineering and assaying of cytochrome P450 biocatalysts. Anal Bioanal Chem 392:1059–1073

Richhardt J, Larsen M, Meinhardt F (2010) An improved transconjugation protocol for *Bacillus megaterium* facilitating a direct genetic knockout. Appl Microbiol Biotechnol 86:1959–1965

Safayhi H, Rall B, Sailer ER, Ammon HP (1997) Inhibition by boswellic acids of human leukocyte elastase. J Pharmacol Exp Ther 281:460–463

Sancho J (2006) Flavodoxins: sequence, folding, binding, function and beyond. Cell Mol Life Sci 63:855–864

Schmitz D, Zapp J, Bernhardt R (2012) Hydroxylation of the triterpenoid dipterocarpol with CYP106A2 from *Bacillus megaterium*. FEBS J 279:1663–1674

Sheng H, Sun H (2011) Synthesis, biology and clinical significance of pentacyclic triterpenes: a multi-target approach to prevention and treatment of metabolic and vascular diseases. Nat Prod Rep 28:543

Sielaff B, Andreesen JR (2005) Kinetic and binding studies with purified recombinant proteins ferredoxin reductase, ferredoxin and cytochrome P450 comprising the morpholine mono-oxygenase from *Mycobacterium* sp. strain HE5. FEBS J 272:1148–1159

Siemoneit U, Hofmann B, Kather N, Lamkemeyer T, Madlung J, Franke L, Schneider G, Jauch J, Poeckel D, Werz O (2008) Identification and functional analysis of cyclooxygenase-1 as a molecular target of boswellic acids. Biochem Pharmacol 75:503–513

Smillie RM (1965) Isolation of two proteins with chloroplast ferredoxin activity from a blue-green alga. Biochem Biophys Res Commun 20:621–629

Sticht H, Rösch P (1998) The structure of iron-sulfur proteins. Prog Biophys Mol Biol 70:95–136

Sussman MD, Vary PS, Hartman C, Setlow P (1988) Integration and mapping of *Bacillus megaterium* genes which code for small, acid-soluble spore proteins and their protease. J Bacteriol 170:4942–4945

Syrovets T, Büchele B, Gedig E, Slupsky JR, Simmet T (2000) Acetyl-boswellic acids are novel catalytic inhibitors of human topoisomerases I and IIalpha. Mol Pharmacol 58:71–81

Syrovets T, Büchele B, Krauss C, Laumonnier Y, Simmet T (2005) Acetyl-boswellic acids inhibit lipopolysaccharide-mediated TNF-alpha induction in monocytes by direct interaction with IkappaB kinases. J Immunol 174:498–506

Tausch L, Henkel A, Siemoneit U, Poeckel D, Kather N, Franke L, Hofmann B, Schneider G, Angioni C, Geisslinger G, Skarke C, Holtmeier W, Beckhaus T, Karas M, Jauch J, Werz O (2009) Identification of human cathepsin G as a functional target of boswellic acids from the anti-inflammatory remedy frankincense. J Immunol 183:3433–3442

Urlacher VB, Eiben S (2006) Cytochrome P450 monooxygenases: perspectives for synthetic application. Trends Biotechnol 24:324–330

Urlacher VB, Girhard M (2012) Cytochrome P450 monooxygenases: an update on perspectives for synthetic application. Trends Biotechnol 30:26–36

Vary PS, Biedendieck R, Fuerch T, Meinhardt F, Rohde M, Deckwer WD, Jahn D (2007) *Bacillus megaterium*-from simple soil bacterium to industrial protein production host. Appl Microbiol Biotechnol 76:957–967

Virus C, Lisurek M, Simgen B, Hannemann F, Bernhardt R (2006) Function and engineering of the 15beta-hydroxylase CYP106A2. Biochem Soc Trans 34:1215–1218

Werck-Reichhart D, Feyereisen R (2000) Cytochromes P450: a success story. Genome Biol. 1:REVIEWS3003

Werz O, Siemoneit U, Henkel A, Jauch J, Kather N Use of boswellic acids and synthetic boswellic acid derivatives for inhibiting microsomal prostaglandin E2 synthase and cathepsin G. Ger. Offen. (2009) DE 102008015607 A1 20091015

Whitehouse CJC, Bell SG, Wong LL (2012) P450(BM3) (CYP102A1): connecting the dots. Chem Soc Rev 41:1218–1260

Wittchen KD, Meinhardt F (1995) Inactivation of the major extracellular protease from *Bacillus megaterium* DSM319 by gene replacement. Appl Microbiol Biotechnol 42:871–877

Zehentgruber D, Hannemann F, Bleif S, Bernhardt R, Lütz S (2010) Towards preparative scale steroid hydroxylation with cytochrome P450 monooxygenase CYP106A2. ChemBioChem 11:713–721

Zheng M, Doan B, Schneider TD, Storz G (1999) OxyR and SoxRS regulation of fur. J Bacteriol 181:4639–4643